JOURNAL OF Applied Polymer SCIENCE

Melt Spinning of PVDF Fibers with Enhanced β Phase Structure

Zengwei Guo,[1] Erik Nilsson,[1,2] Mikael Rigdahl,[2] Bengt Hagström[1,2]
[1]Swerea IVF, Department of Textile and Plastics, Box 104, Mölndal SE-431 22, Sweden
[2]Department of Materials and Manufacturing Technology, Chalmers University of Technology, 412 96 Göteborg, Sweden
Correspondence to: Z. Guo (E-mail: zengwei.guo@swerea.se)

ABSTRACT: Polyvinylidene fluoride (PVDF) fibers with a high amount of β phase crystal structure were prepared by melt spinning. With this technique, the cold drawing process is critical and efficient when aiming for a high amount of β phase. During the cold drawing process, more than 80% of the originally formed α phase crystal structure was converted into the β phase structure. In addition, the incorporation of 0.01 wt % of amino-modified double wall carbon nanotube (NH_2-DWCNT) could further enhance the β phase content in the PVDF fibers. FTIR and DSC studies showed that the addition of NH_2-DWCNT to PVDF fibers could increase both the total crystallinity and β phase fraction in PVDF. The addition of nanoclay was found to be less efficient in this respect.

KEYWORDS: clay; fibers; nanotubes; graphene and fullerenes; textiles

Received 7 December 2012; accepted 30 April 2013; Published online 00 Month 2013
DOI: 10.1002/app.39484

INTRODUCTION

Polyvinylidene fluoride (PVDF) has attracted the attention of several researchers since Kawai found its piezoelectric properties in 1969.[1] Although PVDF shows a lower piezoelectric coefficient in comparison with traditional piezoelectric materials, such as ceramics and single crystal, it is still preferred as a piezoelectric material in many applications due to its low cost and high flexibility.[2,3]

PVDF is a semi-crystalline polymer and can crystallize in five different forms, which involves three different chain conformation, namely, TGTG′ (T-*trans*, G-*gauche*$^+$, G′-*gauche*$^-$) for non-polar α and δ phases, TTTT for the polar β phase, and TTTGTTTG′ for the polar γ and ε phases.[4,5] In all these five phases, the β phase is the most polar phase and exhibits the spontaneous polarization. Once this β phase crystal is poled, it could convert the mechanical deformation into electric energy and vice versa (piezoelectric activity).[6] Therefore, in order to obtain excellent piezoelectric properties, the amount of β phase in PVDF should be as high as possible. Unfortunately, the oriented β phase crystal is not thermodynamically stable because of the high repulsion force between the adjacent CF_2 groups. The non-polar α phase crystal, however, is the most thermodynamically stable polymorph. It directly forms from the cooling of the polymer melt without any need to control the conditions. Technically, when PVDF pre-forms (films or fibers) are produced from PVDF melt, the α phase constitutes the dominating crystalline phase in the PVDF. In order to achieve a high amount of β phase, the PVDF pre-forms are usually drawn to a high draw ratio thus converting the originally formed α phase to β phase crystal.[7,8]

Recently, two other approaches were investigated in order to enhance the formation of the β phase in PVDF. One is to add organically modified nanoclay (layered silicates), the other is to incorporate organically modified carbon nanotubes (CNTs). Priya et al.[9] reported on the addition of organically modified nanoclay into PVDF in 2002. They found that the presence of such nanoclay in PVDF/nanoclay composite could enhance the β phase formation of PVDF. Since then, the study of nanofillers as β phase inducing agent in PVDF has become intensive.[10,11] A few years later, Levi et al.[12] reported that both single wall carbon nanotubes (SWCNT) and multi wall carbon nanotubes (MWCNT) can significantly enhance the β phase in PVDF at very low nanofiller loadings. Quite recently, Lund et al.[13] also found that the incorporation of double wall carbon nanotubes (DWCNT) can facilitate the β phase crystallization in PVDF.

Flexible polymeric piezoelectric fibers have significant potential in the field of smart textiles and flexible sensors and actuators. One of our main aims is to manufacture PVDF fibers with piezoelectric activity by a conventional melt spinning process. To achieve this goal, the preparation of PVDF fibers with a high amount of β phase crystal structure is critical. Several research groups reported that the cold drawing, which is drawing the

Additional Supporting Information may be found in the online version of this article.

fibers at a temperature below the melting point, is an important step in the melt spinning of PVDF fibers reaching a high content of the β phase structure. The cold drawing can enhance the β phase through transformation of originally formed α phase. The total degree of crystallinity, however, is not affected. In this study, we will investigate the efficiency of using cold drawing in the preparation of PVDF fiber enriched in β phase structure. In the mean time, two different kinds of nanofillers were tested as the β phase inducing agents for the enhancement of the β phase structure in PVDF fibers. An attempt to prepare PVDF fibers with the high β phase structure by combination of the cold drawing and incorporation of a β phase inducing agent will be also reported. As far as we know, this is first time that the cold drawing and incorporation of the β phase inducing agent are systematically studied in the preparation of PVDF fibers with the enhanced β phase structure.

EXPERIMENTAL

Materials

PVDF with brand name Solef 1010 was from Solvay Solexis (Milan, Italy) in pellet form. The melt flow index (MFI) of Solef 1010 is 2 g/10 min at a load of 2.16 kg (or 6 g/10 min at a load of 5 kg), at 230°C. Nanoclay with brand name Perkalite F100 was purchased from Akzo Nobel Polymer Chemicals B.V. (Belgium). Perkalite F100 is an organically modified synthetic layered double hydroxide. CNT used in this study were amino-modified DWCNT (NH_2-DWCNT) and obtained from Nanocyl S.A. (Belgium). The average diameter of DWCNT is around 3.5 nm and the length is several microns. The carbon purity of NH_2-DWCNT is above 90%; the rest of less than 10% is metal oxide impurity. The concentration of amino group functionalized on DWCNT is around 0.5 wt %. Epolene E43 was a maleic anhydride grafted polypropylene (PP) oligomer and purchased from Eastman Chemical Corporation. The weight average molecular weight (M_w) and number average molecular weight (M_n) of Epolene E43 are 11,200 and 3850, respectively. The concentration of the grafted maleic anhydride is 8 wt %. PVDF with 5 wt % of CNT was Hyperion PVDF/CNT masterbatch which was purchased from Hyperion Catalysis International, Inc.. The PVDF in Hyperion masterbatch is Solef 1010. Sodium dodecyl sulfate (SDS) was obtained from Sigma-Aldrich with a purity of 98.5%.

Preparation of the Intercalated/Exfoliated Nanoclay

A 4 g of Epolene E43 was added into 100 mL xylene at 100°C. After the Epolene E43 was completely dissolved, 1 g Perkalite F100 was added to the solution and stirred at 100°C for 1 h. Then, 100 mL of acetone was added into the flask to precipitate the Perkalite F100 and Epolene E43 mixture. The precipitation was collected by filtration and washed by excess acetone. The collected Perkalite F100 and Epolene E43 mixture was dried at 80°C under vacuum for overnight.

Preparation of the NH_2-DWCNT Suspension

A 0.04 g NH_2-DWCNT was dispersed into 40 mL deionized water which contained 0.6 wt % of sodium dodecyl sulfate (SDS) surfactant. The NH_2-DWCNT suspension was first sonicated for 15 min in a tip sonicator, and then transferred to a bath sonicator and continued sonication for another 2 h. The sonicated NH_2-DWCNT suspension was centrifuged for 10 min at a speed of 2000 rpm. The supernatant was collected.

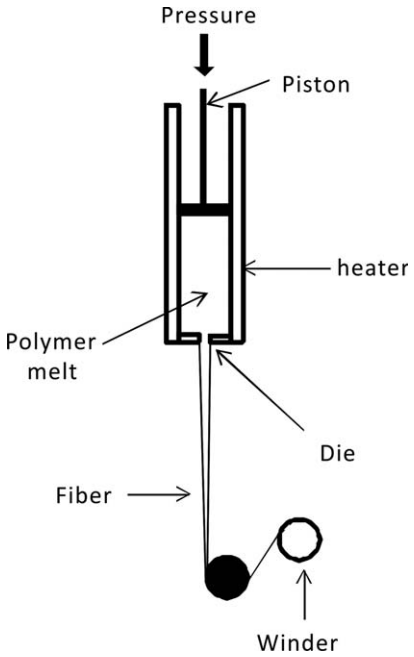

Figure 1. Melt spinning of PVDF and PVDF nanocomposite fibers in capillary rheometer.

Ultraviolet–Visible Spectroscopy (UV–VIS) Measurements

The UV/VIS absorption spectra of NH_2-DWCNT supernatant were recorded with a Specord 200 PLUS from Analytik Jena, using plastic cuvettes with a path length of 1 cm. The UV/VIS spectrum of NH_2-DWCNT supernatant can be seen in Support Information (Supporting Information Figure S1).

Compounding PVDF with NH_2-DWCNT and Nanoclay

PVDF was compounded with NH_2-DWCNT and nanoclay at 200°C in a Brabender kneader (AEV 651 from Brabender, Germany), respectively. The rotation speed was 100 rpm. In case of NH_2-DWNT, 30 g of PVDF pellets was first melt in the Brabender kneader and then 17.5 mL of NH_2-DWCNT suspension was injected into the mixing chamber in 2 min. The PVDF and NH_2-DWCNT were continuously compounded for another 5 min. In case of nanoclay, 30 g of PVDF was first melt in the Brabender kneader and then 15 mg of Epolene E43 modified nanoclay was directly added to the mixing chamber. The PVDF and nanoclay mixture was compounded for 5 min.

Melt Spinning of Monofilaments

Melt spinning of PVDF and PVDF nanocomposite fibers was carried out with a CEAST 1000 capillary viscometer (Italy), as schematically shown in Figure 1. The length and diameter of capillary were 10 and 1 mm, respectively. The draw ratio of monofilament applied in the molten state was around 4.

Cold Drawing of PVDF and PVDF Nanocomposite Fibers

The cold drawing of the PDVF and the PVDF nanocomposite fibers were performed in INSTRON (Dual Column Tabletop Universal Testing Systems, 5966 model) with a heating chamber. The drawing temperature was 90°C and the drawing speed was

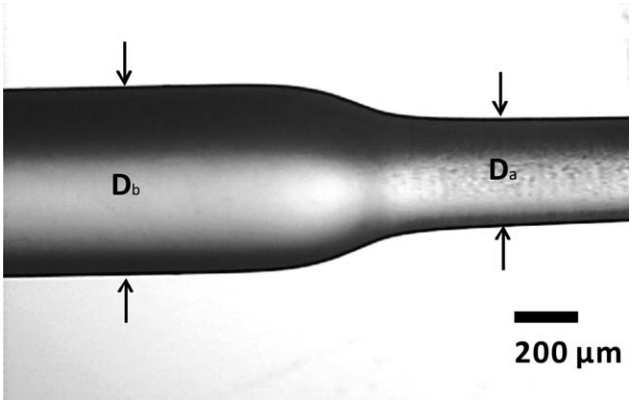

Figure 2. Optical micrograph of a PVDF fiber after cold drawing.

100 mm/min. Before the drawing, fibers were first put into the heating chamber for 1 min. It is well know that the semi-crystalline polymers usually show a necking phenomenon when they are drawn below their melting temperature. The draw ratio formed in the stable neck is called a natural draw ratio (NDR).[14] The cold drawing of PVDF fibers also formed a NDR which could be calculated with the help of optical microscopy as shown in Figure 2,

$$\mathrm{NDR}=\left(\frac{D_b}{D_a}\right)^2 \quad (1)$$

where D_b and D_a are the diameters of the fiber before and after drawing, respectively.

Fourier Transform Infrared Spectroscopy (FTIR) Analysis of the Crystal Structure of PVDF Nanocomposite Fibers

FTIR analysis of PVDF fibers was performed on a Perkin Elmer Spectrum One spectrometer with a resolution of 4 cm^{-1}. The fraction of β phase [F(β)] was calculated based as

$$F(\beta)=\frac{X_\beta}{X_\beta+X_\alpha}=\frac{A_\beta}{1.26A_\alpha+A_\beta} \quad (2)$$

where A_α and A_β in *eq.* (2) are the areas of absorption band at 760 and 840 cm^{-1}, respectively.[8] For each type of PVDF fibers, the $F(\beta)$ was given as an average of six samples.

X-ray Diffraction (XRD)

XRD measurements were performed on XRD Bruker AXS D8 using Cr $K\alpha$ as radiation source. In case of nanoclay and nanoclay/Epolene E43 mixture, samples in the powder form were pressed onto the sample holder. The measured diffraction angle 2θ was in the range from 2° to 20°. The measuring step was 0.1° and measuring time for each step was 10 s. In case of PVDF/CNT composite fibers, fibers were mounted on a flat sample holder using double-sided adhesive tape. The measured diffraction angle 2θ was 20–40°. The increment step was 0.1° and measuring time for each step was 10 s. During the measurements, the sample was rotating at a speed of 30 rpm.

Differential Scanning Calorimetry (DSC)

DSC was carried out with DSC 1 from Mettler Toledo under nitrogen atmosphere. The temperature scans were carried out between 40 and 260°C at a heating rate of 10°C/min. The total crystallinity (TC) of PVDF was determined from the endotherm area using 104.6 J/g as the heat of fusion of 100% crystalline PVDF. The β phase crystallinity [C(β)] was calculated as

$$C(\beta)=TC\times F(\beta). \quad (3)$$

For each type of PVDF fibers, the β phase crystallinity was given as an average of six samples. DSC curves of PVDF fibers were list in Support Information (Supporting Information Figure S2).

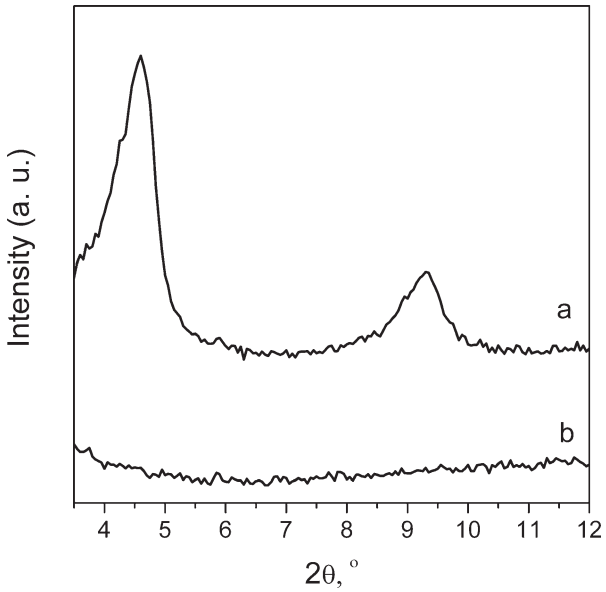

Figure 3. XRD diffractograms of (a) pure nanoclay and (b) nanoclay after being mixed with Epolene E43 solution.

RESULTS AND DISCUSSION

Preparation of Exfoliated/Intercalated Nanoclay by Solution Method

In order to get a homogenous dispersion of nanoclay in the PVDF matrix, the nanoclay should be in the exfoliated state. However, it is difficult to prepare the exfoliated nanoclay/PVDF nanocomposite since nanoclay is hydrophilic whereas PVDF is hydrophobic. To facilitate the exfoliation of nanoclay in PVDF, the nanoclay was first mixed with maleic anhydride grafted PP (Epolene E43) which is often used as compatibilizer for the preparation of nanoclay/PP composites by melt compounding.[15] In the melt compounding process, Epolene E43 can diffuse into the galleries of nanoclay and expand the interlayer distance. Therefore, the exfoliation of nanoclay in PP becomes possible to achieve. In this study, Epolene E43 was dissolved in xylene at 100°C. This enhanced the mobility of Epolene E43 molecules and thus accelerated the diffusion of Epolene E43 into nanoclay. A few minutes after the addition of nanoclay, the Epolene E43 solution started to gelate. This gelation confirms the diffusion of Epolene E43 into nanoclay galleries and the change of the nanoclay structure. Furthermore, the nanoclay and Epolene E43 mixture as well as pure nanoclay powder were analyzed by XRD. In Figure 3(a), two intensive diffraction peaks at 2θ = 5.1° and 10.3° in the XRD pattern of pure nanoclay are clearly observed. While, these two diffractions peaks disappear

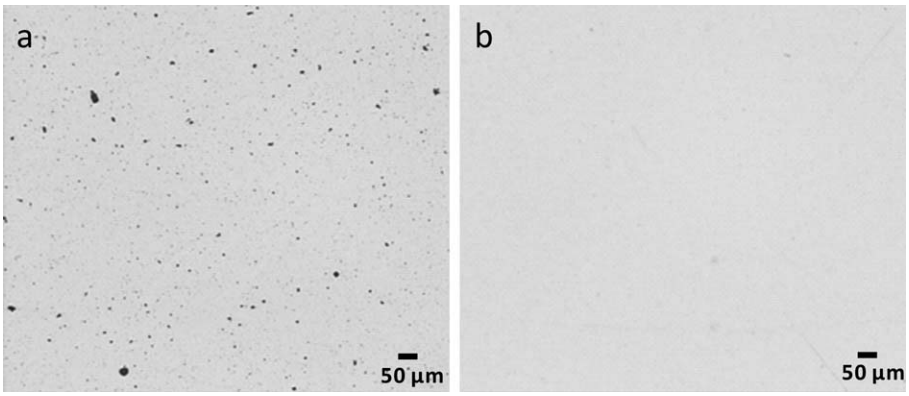

Figure 4. Optical micrographs of the NH_2-DWCNT suspension; (a) is the NH_2-DWCNT suspension before centrifugation and (b) is the supernatant.

in the diffractogram for the nanoclay–Epolene E43 mixture. This indicates that nanoclay probably was completely exfoliated in Epolene E43 solution or intercalated to a significant extent that makes the Bragg angle too small to be measured.

Preparation of the NH_2-DWCNT Suspension

NH_2-DWCNT was, as described, dispersed in water with the help of SDS surfactant. After more than 2 h sonication, a black suspension of NH_2-DWCNT was obtained. This suspension, however, was not very homogenous as revealed by optical microscopy [Figure 4(a)]. Several NH_2-DWCNT aggregates in micrometer size could easily be observed. The presence of these NH_2-DWCNT aggregates in the suspension is negative with regard to the dispersion since the NH_2-DWCNT aggregates are very hard to break in the following melt compounding process. At the end, a poor dispersion of NH_2-DWCNT will reduce the surface interactions between PVDF and NH_2-DWNTs, which in return reduces the possibility of attaining a β phase enhancement. In addition, the presence of NH_2-DWCNT aggregates can lead to poor spinnability and drawability since the diameter of obtained PVDF fibers was of the micrometer scale. In order to remove the large NH_2-DWCNT aggregates, the sonicated NH_2-DWCNT suspension was centrifuged for 10 min, and the supernatant was collected for preparation of PDVF/NH_2-DWCNT composites. The NH_2-DWCNT in the supernatant constitutes a very homogenous dispersion. No large NH_2-DWCNT aggregates could be found in the supernatant as shown in Figure 4(b).

The concentration of NH_2-DWCNT in the supernatant was determined by UV–VIS spectroscopy based on Beer–Lambert's law,

$$A = \varepsilon\ C\ l \tag{4}$$

where A is the absorbance at the wavelength of 690 nm, ε is the extinction coefficient at the same wavelength (ε_{690nm} = 32.3 mL mg^{-1} cm^{-1}), C is the concentration of NH_2-DWCNT, and l is the light path length.[16] According to *eq.* (4), the concentration of NH_2-DWCNT in the supernatant is 0.171 mg/mL.

Transformation of α to β Phase in the PVDF Fiber by Cold Drawing

The α phase is usually dominating phase in melt-spun PVDF fibers since the PVDF fibers are directly cooled from polymer melt without any control. In order to obtain piezoelectric properties of PVDF fibers, a cold drawing is necessary. Here, the melt-spun PVDF fibers were cold drawn to a natural draw ratio of around 3.3.

FITR is a well-known method to analyze and quantitatively determine the crystal structure in PVDF.[8,17] According to the literature, the vibrational bands at 764, 796, 855, and 976 cm^{-1} are characteristic bands of the α phase whereas the vibrational band at around 840 cm^{-1} devotes the β phase in PVDF. As shown in FTIR spectrum for undrawn PVDF fibers in Figure 5(a), the absorption bands corresponding to α phase clearly appeared in the FTIR spectrum and these bands were very intensive. In contrast, the absorption band which is attributed to the β phase was weak. This indicates that α phase is dominant in the undrawn PVDF fiber. However, after cold drawing, the intensity of β phase vibrational band at 840 cm^{-1} increased significantly. It became a dominate band in Figure 5(b). The absorption bands ascribed to the α phase became weaker, especially, the bands at 796 and 976 cm^{-1} which almost disappeared.

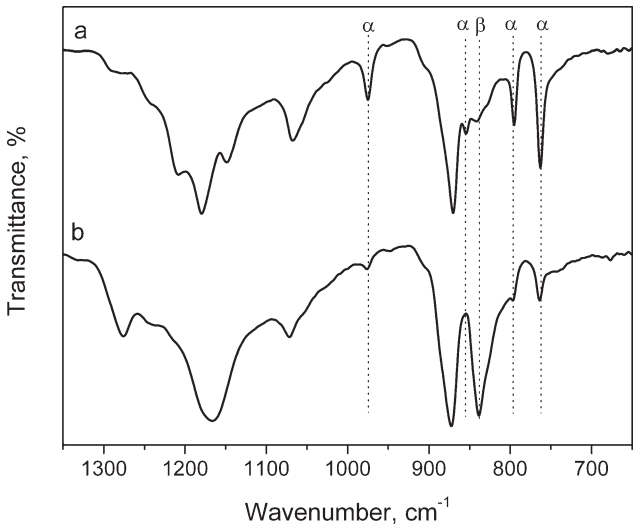

Figure 5. FTIR spectra of PVDF fibers, (a): PVDF fiber without cold drawing; (b): PVDF fiber with cold drawing.

Table I. Crystallinity of Different PVDF Fibers

Name	Natural draw ratio	Total crystallinity (%)	$F(\beta)$ (%)	β phase crystallinity (%)
PVDF fibers	3.48 ± 0.13	44.74 ± 1.56	89.18 ± 2.07	39.95 ± 2.32
PVDF/nanoclay fibers	3.31 ± 0.18	46.84 ± 0.45	89.83 ± 3.82	42.09 ± 2.19
PVDF/CNTs fibers	3.37 ± 0.16	48.60 ± 0.66	93.72 ± 2.26	45.58 ± 1.72

Using *eq.* (2), the β phase fraction, given by $F(\beta)$, was about 8% for undrawn fibers, whereas for the drawn fibers with a natural draw ratio of 3.3, the $F(\beta)$ was around 89%. It means that more than 80% of originally formed α phase was converted to the piezoelectric active β phase by the cold drawing. Therefore, the cold drawing is necessary and efficient route to prepare PVDF fibers with a high β phase concentration.

Influence of Nanofillers on the Enhancement of β Phase in PVDF Fibers

PVDF/NH_2-DWCNT and PVDF/nanoclay composite fibers with a nanofiller concentration of 0.01 wt % were prepared using the capillary rheometer. This concentration is chosen according to the work by Lund et al.[13] After the cold drawing, the PVDF/NH_2-DWCNT and PVDF/nanoclay composite fibers with a natural draw ratio of around 3.3 were analyzed by DSC, FTIR, and XRD. As reference, a pure PVDF fiber was also prepared at identical conditions.

As presented in Table I, the total crystallinity of pure PVDF fibers was around 44.7 ± 1.9%. When 0.01 wt % of nanoclay and NH_2-DWCNT were incorporated into the PVDF fibers, the total crystallinity increased to 46.8 ± 0.5% and 48.6 ± 0.7%, respectively. This indicates that the incorporation of nanofillers can increase the total crystallinity of PVDF. However, compared with nanoclay, NH_2-DWCNT was more efficient on the increase of crystallinity of PVDF. Moreover, the fraction of β phase given by $F(\beta)$ in the PVDF/NH_2-DWCNT composite fibers was slight increased, which was not observed in the PVDF/nanoclay composite fibers. The calculated β phase crystallinity in the PVDF/NH_2-DWCNT composite fibers was around 45.6%, which was more than 3% higher than that of PVDF/nanoclay composites.

The NH_2-DWCNT enhanced β phase structure in PVDF fiber was further confirmed by XRD measurements as shown in Figure 6. For pure PVDF fibers after the cold drawing [Figure 6(a)], two diffraction peaks could clearly be identified: one is a strong diffraction peak at $2\theta = 30.7°$, the other is a broad and weaker peak at $2\theta = 27.8°$. The strong diffraction at $2\theta = 30.7°$ is assigned to the (110)/(200) reflection planes of β phase crystal structure in PVDF,[18,19] whereas the broad peak at the lower diffraction angle is one of characteristic diffraction peaks of α phase crystal, which corresponds to the (200) reflection plane of the α phase.[18,19] When the CNTs were added into the PVDF fibers, the β phase diffraction peak became more intense. In contrast, the α phase peak at $2\theta = 27.8°$ turned into a broad shoulder and almost disappeared. This indicates that the presence of CNTs in PVDF fiber enhances β phase after the fibers have been cold drawn.

Further studies revealed that the enhancement effect can be greatly improved using a higher CNT content. When 5 wt % of CNT was incorporated into the PVDF fiber, the absorption band at 840 cm^{-1} became very intensive even when PVDF fibers were directly cooled from polymer melt without the cold drawing (Figure 7). According to *eq.* (2), the β phase

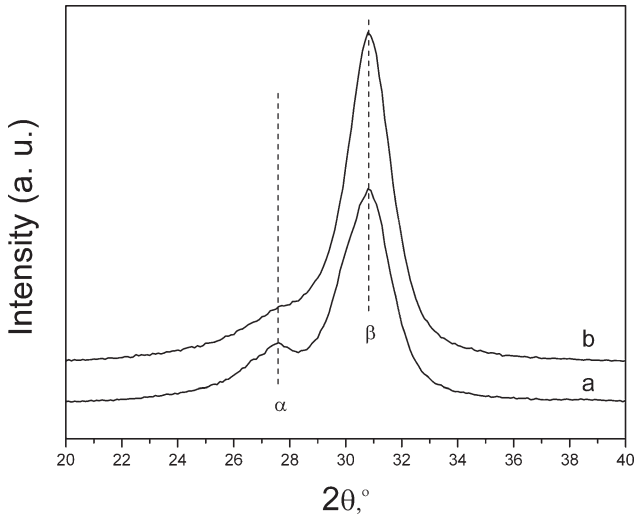

Figure 6. XRD diffractograms of PVDF fibers. (a) PVDF fibers without NH_2-DWNT; (b) PVDF fibers with incorporation of 0.01 wt % of NH_2-DWCNT.

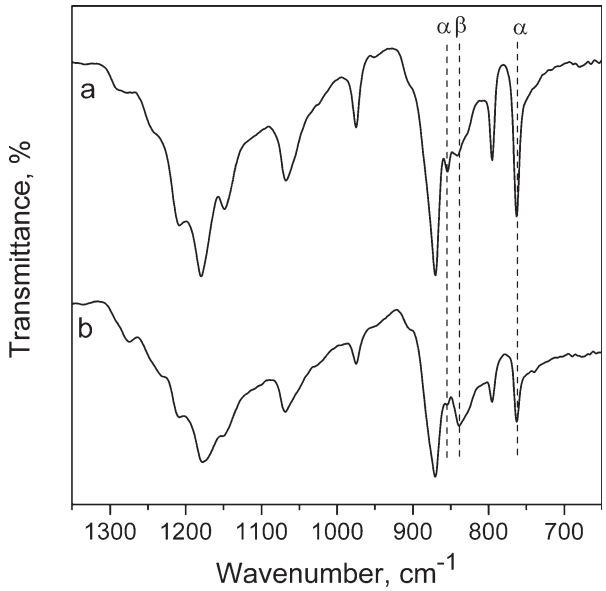

Figure 7. FTIR spectra of PVDF fibers, (a): pure PVDF fibers; (b): PVDF fiber with 5 wt % of CNT. These two types of fibers were not cold drawn.

concentration in these undrawn PVDF/CNT composite fibers reached around 65%. This value is more than eight times higher than that of undrawn pure PVDF fibers. This indicates that the presence of a high amount of CNT in PVDF fiber can significantly suppress the α phase and thus enhance the formation of the β phase.

Recently, several other groups have also confirmed the observation of β phase enhancement by incorporation of CNT.[20–22] To explain this phenomenon, we now propose the following: It is well known that CNTs are electron-rich molecules.[23,24] Any electron-deficient molecule can interact with them and form donor–accepter complexes, in the same way as electron-rich molecules form π–π complexes.[25,26] During the melt compounding, the PVDF chains are very mobile and can effectively wrap over individual CNT.[26] Their fluorine groups are strongly attracted by the delocalized π-electron clouds on the CNTs and can thus establish donor–acceptor complexes. In these complexes, the mobility of PVDF chains is limited due to the strong interaction between delocalized π-electron clouds on CNTs and electrophilic fluorine groups on the PVDF chains. Therefore, establishing these complexes induces a very thin layer wrapping around CNTs in which PVDF chains are guided by CNTS to form the TTTTT conformation. In the cooling process, PVDF in the absence of CNTs crystallizes into α phase conformation, which is thermodynamically favored over β phase conformation at room temperature.[27] However, for PVDF in the presence of CNT, the PVDF chains in these thin layers on the CNTs can directly crystallize into the thermodynamically unfavored β phase because the interaction in the donor–acceptor complexes limits the mobility of the PVDF chains in these thin layers and prohibits the conversation of β phase to α phase. It has been found that some very thin layers with thickness of 10–30 nm were formed around the CNTs and these thin layers showed strong interaction with CNTs.[28] At this point, the CNTs work as β phase inducing templates to enhance β phase structure in PVDF on the molecular level. Furthermore, the added CNTs provide a huge interfacial area which in turn gives numerous sites for the formation of thin PVDF layers with β phase conformation. This is also the reason why the enhancement is more obvious at higher CNT concentration. However, the high nanofiller concentration can significantly reduce the spinnability of polymers.[29] Therefore, the application of CNT to enhance β phase structure in PVDF fibers should be limited to the low incorporation level.

CONCLUSIONS

To conclude, PVDF fibers with the high amount of β phase structure can be prepared by a combination of cold drawing and using CNTs as a β phase enhancing agent. The cold drawing is efficient for obtaining PVDF fibers with a high amount of β phase structure. It can convert around 80% of the originally formed α phase crystal to β phase structure at a natural draw ratio of 3.3. The incorporation of CNT could further enhance the β phase in PVDF fibers even at a concentration of CNT of 0.01 wt %. This kind of enhancement is different from the enhancement induced by cold drawing. The enhancement induced by incorporation of CNT is seen as the result of an increase of both the total crystallinity and the β phase fraction in PVDF fibers.

A more significant β phase enhancement can be obtained at high CNT concentration. However, the high CNT concentration will lead to poor spinnability of PVDF. Furthermore, a high CNT concentration in PVDF will increase the electrical conductivity of PVDF which will result in a loss of the piezoelectric activity of PVDF. An optimum concentration of CNT at which the CNT could maximize enhancement effect without reducing the piezoelectric activity and spinnability is aimed for in our further studies.

ACKNOWLEDGMENTS

We gratefully acknowledge the financial support by the Swedish Foundation for Strategic Research (SSF) and the Swedish Governmental Agency for Innovation Systems (Vinnova).

REFERENCES

1. Kawai, H. *Jpn. J. Appl. Phys.* **1969**, *8*, 975.
2. Sessier, G. M. *J. Acoust. Soc. Am.* **1981**, *70*, 1596.
3. Anton, S.; Sodano, H. *Smart Mater. Struct.* **2007**, *16*, R1.
4. Gregorio, R. *J. Appl. Polym. Sci.* **2006**, *100*, 3272.
5. Yousefi A. A. *Iran. Polym. J.* **2011**, *20*, 725.
6. Ramos, M.; Correia, H.; Lanceros-Mendez, S. *Comput. Mater. Sci.* **2005**, *33*, 230.
7. Humphreys, J.; Ward, I. M. *J. Appl. Polym. Sci.* **1985**, *30*, 4069.
8. Salimi, A.; Yousefi, A. A. *Polym. Test.* **2003**, *22*, 699.
9. Priya, L.; Jog, J. P. *J. Polym. Sci. Part B: Polym. Phys.* **2002**, *40*, 1682.
10. Ramasundaram, S.; Yoon, S.; Kim, K.; Park, C. *J. Polym. Sci. Part B: Polym. Phys.* **2008**, *46*, 2173.
11. Yu, L.; Cebe, P. *Polymer,* **2009**, *50*, 2133.
12. Levi, N.; Czerw, R.; Xing, S.; Lyer, P.; Carroll, D. l. *Nano Lett.* **2004**, *4*, 1267.
13. Lund, A.; Gustafsson, C.; Bertilsson, H.; Rychwalski, R. *Compos. Sci. Technol.* **2011**, *71*, 222.
14. Seguela, R. *Macromol. Mater. Eng.* **2007**, *292*, 235.
15. Ton-that, M. T.; Perrin-Sarazin, F. P.; Cole, K. C.; Bureau, M. N.; Denault, J. *Polym. Eng. Sci.* **2004**, *44*, 1212.
16. Jeong, S. H.; Kim, K. K.; Jeong, S. J.; An, K. K.; Lee, S. H.; Lee, Y. H. *Synt. Met.* **2007**, *157*, 570.
17. Boccacio, T.; Bottino, A.; Capannelli, G.; Piaggio, P. *J. Membr. Sci.* **2002**, *210*, 315.
18. Wang, Y.; Cakmak, M.; White, J. L. *J. Appl. Polym. Sci.* **1985**, *30*, 2615.
19. Lund, A.; Hagström, B. *J. Appl. Polym. Sci.* **2010**, *116*, 2685.
20. Mago, G.; Fisher, F. T.; Kalyon, M. *J. Nanosci. Nanotechnol.* **2009**, *9*, 3330.
21. Huang, X.; Jiang, P.; Kim, C.; Liu, F.; Yin, Y. *Eur. Polym. J.* **2009**, *45*, 377.

22. He, L.; Xu, Q.; Hua, C.; Song, R. *Polym. Compos.* **2010**, *31*, 921.

23. Zhang, J.; Lee, J. K.; Wu, Y.; Murray, W. *Nano Lett.* **2003**, *3*, 403.

24. Li, H.; Zhou, B.; Lin, Y.; Gu, L.; Wang, W.; Shiral Fernando, K.; Kumar, S.; Allard, L. F.; Sun, Y. *J. Am. Chem. Soc.* **2004**, *126*, 1014.

25. Baskaran, D.; Mays, J. M.; Bratcher, M. S. *Chem. Mater.* **2005**, *17*, 3389.

26. Zhang, Z.; Zhang, J.; Chen, P.; Zhang, B.; He, J.; Hu, G. *Carbon* **2006**, *44*, 692.

27. Satyanarayana, K. C.; Bohlen, M.; Lund, A.; Rychwalski, R.; Bolton, K. *Polymer* **2012**, *53*, 1109.

28. Yuan, J.; Yao, S.; Dang, Z.; Sylvestre, A.; Genestoux, M.; Bai, J. *J. Phys. Chem. C* **2011**, *115*, 5515.

29. Stråat, M.; Toll, S.; Boldizar, A.; Rigdal, M.; Hagström, B. *J. Appl. Polym. Sci.* **2011**, *119*, 3264.